View metadata, citation and similar papers at core.ac.uk

brought to you by CORE

provided by Sound Ideas

Honors Program

Honors Program Theses

University of Puget Sound *Year* 2015

Insights into the evolution of the Great Plains grassland ecosystem over the last 5 million years from paleotemperature and paleovegetation records

Anne Fetrow
University of Puget Sound, afetrow@pugetsound.edu

This paper is posted at Sound Ideas.
http://soundideas.pugetsound.edu/honors_program_theses/13

UNIVERSITY OF PUGET SOUND

Insights into the evolution of the Great Plains grassland ecosystem over the last 5 million years from paleotemperature and paleovegetation records

Anne Fetrow

Coolidge Otis Chapman Honors Senior Thesis

April 20th, 2015

Table of Contents

Abstract

Over the last 10 million years, the Great Plains transitioned to the modern C_4 grass dominated ecosystem. Well-preserved late Miocene to Holocene fossils and paleosols make the Meade Basin in southwest Kansas, USA a unique place to determine how paleoenvironmental conditions changed during C_4 grassland evolution. $\delta^{18}O$ values of paleosol carbonates ($\delta^{18}O_{carb}$) in the Meade Basin decreased from the Miocene to Holocene while $\delta^{13}C$ values increased; these trends were interpreted as an increase in temperature and/or in aridity coincident with an increase of C_4 grass biomass on the landscape. Estimating temperature from $\delta^{18}O_{carb}$ is complicated, however, by the role of source water $\delta^{18}O$ ($\delta^{18}O_{water}$) values in $\delta^{18}O_{carb}$ values. Thus, we used carbonate clumped isotope (Δ_{47}) thermometry of paleosol carbonate nodules to develop independent paleotemperature estimates and estimated $\delta^{18}O_{water}$ by combining temperature and $\delta^{18}O_{carb}$ values.

Preliminary temperature estimates (5-1.8 Ma) in the Meade Basin range from 17°C to 24°C with no systematic change through time, when compared to the modern mean annual (14°C) and warm season (24°C) temperatures. In contrast, $\delta^{18}O_{water}$ values increased through time. We preliminarily suggest that local/regional temperature change was not the primary factor that drove grassland ecosystem evolution in the Meade Basin, while increasing $\delta^{18}O_{water}$ values suggest increased aridity may have been a bigger influence on C_4 biomass and faunal changes, although we cannot rule out atmospheric CO_2 (pCO_2) changes. In addition, Δ_{47} temperatures and $\delta^{18}O_{water}$ values may reflect numerous factors besides air temperature and aridity changes, respectively, including depositional environment differences, soil type/depth, and source water changes. Additional analyses and detailed organic biomarker records currently underway will help further constrain the roles of paleoenvironmental factors in C_4 grassland expansion.

Introduction

Over the last 10 million years (m.y.), the Great Plains ecosystem in North America has evolved into the modern grassland ecosystem characterized by an understory dominated by C_4 grasses (Fox et al., 2011a; Edwards et al., 2010; Still et al., 2010; van Fischer et al., 2008; Sage et al., 2004; Cerling et al., 1997; Ehleringer et al., 1997; Ehleringer et al., 1991). C_4 dominated grassland ecosystems are pervasive across the globe and constitute approximately 25% of gross primary productivity on Earth today while comprising less than 4% of all terrestrial plant species (Edwards et al., 2011; Str□mberg et al., 2011; Edwards et al., 2010; Cowling et al., 2007; Still et al., 2003). In general, modern C_4 grass biomass varies latitudinally across the Great Plains, with the highest C_4 biomass in Texas (>90%) and lowest in North Dakota (<10%). These grassland ecosystems have received considerable attention in the past several decades because of their important ecological, geochemical, and evolutionary influence on the geologic record, and their economic significance today. Determining the reason for the development of a C_4 dominated grassland ecosystem will provide critical information to better understand environmental interactions that occurred over the last 10 m.y. in the Great Plains ecosystem.

Stable isotope analyses of ungulate tooth enamel, soil carbonates, carbonate cements, plant lipids, and phytolith assemblages provide insight into the evolution of the Great Plains grasslands. These datasets suggest the region evolved from a C_3 grass dominated landscape to an ecosystem dominated by C_4 grasses along with distinct shifts in mammalian morphology and community assemblage (Fox et al., 2011a; McInerney et al., 2011; Passey et al., 2010; Martin et al., 2008; Fox and Koch, 2004; Fox and Koch, 2003; Passey et al., 2002; Martin et al., 2000; Cerling et al., 1997). For example, the tooth crown height of grazers, such as horses, increased in response to C_4 forage availability (Passey et al., 2002), and there were distinct episodes of

resorting within the small mammal community (Martin et al., 2008). The exact timing of the evolution of the C_4 photosynthetic pathway remains uncertain in part because of the complex evolution of the clade of grasses, Poaceae, of which C_4 grasses are a part (Fox et al., 2011a). The clade of Poaceae evolved during the Late Cretaceous according to molecular clock (Janssen and Bremer, 2004; Bremer, 2002) and fossil phytolith analyzes (Prasad et al., 2005), however, it is suggested that the timing of the evolution varied across continents because of differing environmental conditions (Fox et al., 2011a). On the North American continent, C_4 grasses are thought to have evolved during the Oligocene (33.9 – 23 m.y.) (Christin et al., 2008; Tipple and Pagani, 2007; Sage, 2004) while the rise in C_4 grasses' ecological dominance did not occur until approximately the Miocene (10-8 Ma) (Fox et al., 2011b; Passey et al., 2002).

The disparity between the timing of the evolution of the C_4 photosynthetic pathway and its dominance within open, grass-dominated ecosystems raises the perplexing question of why C_4 grasses took approximately 20 million years to become ecologically relevant after evolving. The Meade Basin in southwestern Kansas preserves a sequence of fossil-bearing paleosols that capture the past 10 million years of grassland evolution. By 9 Ma, the ecosystem of Meade County was a mixture of C_3 (~80%) and C_4 (~20%) grasses (Fox et al., 2011a). Between 5 m.y. and 2.5 m.y., the ecosystem evolved into the modern state with approximately 78% C_4 grasses biomass (Fox et al., 2011a). Different environmental factors facilitated the C_4 grass expansion, including global temperature change, changes in atmospheric pCO_2, and global and/or local aridification (Fox et al., 2011a/b; Beerling and Royer, 2011; Breecker at al., 2010; Tipple et al., 2010; Cerling et al., 1997; Latorre et al., 1996; Cerling and Quade, 1993). More complete paleoenvironmental records are needed to gain a detailed understanding of the dynamics of C_4 grassland evolution at the local scale.

In order to begin to answer this large paleoenvironmental question, we have developed new paleoclimate records that span the Great Plains C_4 grassland evolution over the past 10 million years. The Meade Basin is a particularly high-quality location to establish this context because of its biostratigraphy, geochronology, sedimentology, and stratigraphy that have been determined from numerous, well-preserved, and accessible outcrops (Fox et al., 2011a/b; Martin et al., 2008; Honey et al., 2005; Martin et al., 2000; Izett and Honey, 1995; Zakrezewski, 1975; Hibbard and Taylor, 1960). In this study, we use stable carbon, oxygen, and "clumped" isotope analysis of paleosol carbonate nodules to reconstruct paleotemperature, paleohydrology, and paleovegetation for the Meade Basin. Within this study, we aim to address the question: do variations in the paleotemperature record correlate with changes in paleovegetation and/or intervals of small mammal change?

Methods and Materials

Meade Basin Field Location

Field sites for this project are located in the Meade Basin, which is a northeast-southwest trending depositional basin located in southwest Kansas in Meade County (Fox et al., 2011a/b; Izett and Honey, 1995). Meade Basin contains late Miocene to Holocene deposits and is approximately 50km in length, extending across the Kansas-Oklahoma border (Figure 1). The Cimarron River and its tributaries downcut the Meade Basin and are the primary cause for extensive exposure of the Meade Basin sedimentary rocks. Deposits are mostly fluvial silts and sands which contain pedogenic carbonate nodules and calcrete zones, small mammal fossils, and are interbedded by generally well-preserved paleosols (Figure 2) (Fox et al., 2011a/b; Martin et al., 2008; Izett and Honey, 1995). The well-understood mammalian biostratigraphy and the presence of the Huckleberry Ridge ash layer (2.06Ma), Cerro Toledo B ashes (1.47-1.23Ma), and Lava Creek B ash (0.64Ma) provide well-resolved ages for the Meade Basin strata (Martin et al., 2003; Fox et al., 2011a).

Sample Collection

Carbonates nodule were collected from paleosols throughout seven sections (Figure 1). Nodules were taken at vertical intervals that ranged from 3 to 277cm and averaged ~35 ± 4.8cm. Each nodule was collected *in-situ* and the stratigraphic height was measured from the base of the section for each. Paleosol sections were trenched using shovels and pick-axes in order to expose fresh surfaces from which to collect samples. Some sections overlapped stratigraphically. For example, the section NNT1 is located at the same geographic location of Raptor 1 (RP1) and is considered to have formed during a portion of the same time period (Figure 2). NNT1 is a thick and carbonate-rich section that was sampled more exhaustively at ~10cm intervals in order to

provide a higher resolution record to distinguish effects of soil depth on different paleoclimate datasets.

Stable Isotope Geochemistry

Carbonate Clumped Isotope (Δ_{47}) Thermometry

Carbonate forms naturally in a variety of settings, and is part of many common minerals, including calcite, dolomite, aragonite, and siderite. During the precipitation process, 'clumping" of heavy isotopes, ^{18}O-^{13}C, in carbonate ions, becomes more pronounced as the temperature decreases during mineral formation (Quade et al., 2013; Huntington et al., 2009; Eiler, 2007; Eiler and Ghosh et al., 2006; Schauble, 2004). This preferential 'clumping' of the heavier and rarer isotopes into the same molecule is thermodynamically favored at cooler temperatures, rather than a random distribution of isotopes (Ghosh et al., 2006; Eiler and Schauble, 2004; Wang et al., 2004). A measurable form of these isotopologues can be produced by digestion of carbonate powder in phosphoric acid to produce CO_2 (Swart et al. 1991). The "clumped" isotopologue of this evolved CO_2 (^{18}O-^{13}C-^{16}O) has a molecular mass of 47 (Ghosh et al., 2006), and is the most abundant of the heavy-substituted isotopologues (Eiler, 2007; Eiler and Schauble, 2004). The inverse relationship between 'clumping' and temperature of carbonate formation is described by Ghosh et al. (2006) and can be used as a paleothermometer. The abundance of mass-47 is expressed as the ratio of measured mass-47 to measured mass-44 ($R^{47}_{sample} = M^{47}_{sample}/ M^{44}_{sample}$) compared to the expected R^{47} value for a stochastic distribution of ^{13}C and ^{18}O isotopes among CO_2 molecules (Eiler, 2007; Eiler and Schauble, 2004): $\Delta_{47} = \left(\frac{R^{47}_{sample}}{R^{47}_{Stochastic}} - 1\right) * 1000$ (1).

Along with Δ_{47} temperature estimates, carbon ($\delta^{13}C$) and oxygen ($\delta^{18}O$) isotope values were determined for each carbonate sample. $\delta^{18}O$ of the water ($\delta^{18}O_w$) from which the mineral

precipitated was calculated from the Δ_{47} temperature estimate and the $\delta^{18}O$ of the carbonate ($\delta^{18}O_c$). Carbon and oxygen stable isotope ratios are reported using delta notation, $\delta = \left[\frac{R_{sample}}{R_{standard}} - 1\right] * 1000$ where R is the molar ratio of the heavy to light isotope of the sample or standard ($R = \frac{heavy}{light}$) and expressed on a permil scale (‰), relative to the Vienna Peedee Belemnite standard composition and Standard Mean Ocean Water (SMOW), respectively.

Sample preparation for isotope analysis

We cut carbonate nodules along the longest axis using a rock saw and polished the cut surfaces using a combination of polishing wheel, sand paper, and polishing glass with varying sizes of grit. From these polished faces, we drilled small areas to create a fine powder using a dental drill under a binocular microscope to a maximum of 1-2mm in depth. This powder was then ground with a mortar and pestle to homogenize the sample. The vast majority for samples appeared homogenous, with no evidence for diagenesis, such as secondary mineral precipitation or recrystallized sections (e.g. large crystals or veins). We carefully drilled powder only from nodule regions with no diagenetic indicators. A selection of samples is shown in figure 7 to demonstrate drilling technique, and the range in nodule mineralogy.

Analytical Procedure

Approximately 10-12mg of the powdered samples was weighed into silver capsules and loaded into a sample carousel fitted to a semi-automated CO_2 gas generation and cleaning system (Passey et al., 2010; Huntington et al., 2009). In this system, carbonate samples and carbonate standards are digested in a bath of phosphoric acid held at 90□C, yielding CO_2 gas. These CO_2 gases, as well as heated gas standards that are prepared beforehand, are cryogenically purified by passing through traps at approximately -60°C to remove water and a poropak-filled gas chromatograph column held at -20°C to remove possible contaminants that have the same

molecular masses as the CO_2 isotopologues of interest (masses 44, 45, 46, 47). Carbonate $\delta^{18}O$ values ($\delta^{18}O_C$) were calculated using the acid digestion fractionation factor of 1.000821 (Swart et al., 1991). Thirteen samples out of 44 show excess mass-48, which is often the result of incomplete cleaning of hydrocarbons or halocarbons which produce potential interference with the Δ_{47} values (Huntington et al., 2009; Ghosh et al., 2006).

Analytical Error and Temperature Estimations

Each CO_2 gas sample was analyzed 5-8 times on the mass spectrometer; each of these acquisitions included 7-10 cycles of sample and reference gas peak determinations with 8-second peak integration times. The average isotope ratios from the 5-8 acquisitions were used to determine the uncorrected Δ_{47} values ($\Delta_{47,\ unc}$) and associated $\delta^{13}C$ and $\delta^{18}O$ values. $\Delta_{47,\ unc}$ values were corrected ($\Delta_{47,corr}$) for non-linearity effects in the mass spectrometer using a heated gas line generated from CO_2 gases heated to 1000°C. Changes in the heated gas line were corrected to instrument conditions during the determination of the original Δ_{47}-temperature calibration using a stretching factor, following the procedure discussed in Huntington et al. (2009) and Passey et al. (2010). For individual gas $\Delta_{47,\ unc}$ values analytical precision ranges from 0.0049‰ to 0.0163‰ (one standard error of the mean (1 s.e.)). Uncertainties for $\Delta_{47,corr}$ values in our data set range from 0.0077‰ to 0.0284‰, which includes error associated with the heated gas line, in addition to the analytical uncertainties of the sample. Heated gases and gases held at 25□C equilibration with deionized water were used to create a transfer function that converted the "in-house" $\Delta_{47,\ unc}$ values to the Absolute Reference Frame (ARF). Two carbonate standards, CIT Carrara marble and TV03, were also analyzed to monitor instrument accuracy and precision during analysis. From the converted Δ_{47} values, temperatures are calculated using the calibration from Ghosh et al. (2006).

Statistical Analyses

Statistical tests were conducted using JMP® v11 (SAS Institute Inc., 2013). We used Levene's test of unequal variance to identify differences in variability of Δ_{47} temperature estimates, $\delta^{18}O$ values, and $\delta^{13}C$ values between sections. Both the temperature estimate and $\delta^{18}O$ value variances were significantly unequal ($p<0.05$) so for these factors we used the nonparametric Welch's ANOVA test to analyze differences among sections. The result of the Levene's test for the $\delta^{13}C$ values was not significant, indicating variances are equal among sections, so we used a parameteric one-way ANOVA to analyze differences in $\delta^{13}C$ values among sections.

Results

Preliminary Temperature Estimates and Variability

The modern mean annual and warm season temperatures for Meade are 14°C and 24°C, respectively (Fox et al., 2011a) (Table 1). Our preliminary temperature estimates for 5 to 1.8 Ma in the Meade Basin range from 17°C to 24°C with no systematic change through time. The average temperature, using the estimates from all of the sections, is 21°C ± 5°C (Figure 3). The Welch's ANOVA test found no significant difference in Δ_{47} temperature estimates between sections. The Levene's test showed significantly different variances among sections ($F_{5,36}$=3.025, p=0.0222), however. The standard deviation of the temperature estimates within a section ranged from 1.338□C to 2.561□C.

$\delta^{18}O_{water}$ values

In contrast to the temperatures, $\delta^{18}O_w$ values increase through time. $\delta^{18}O_w$ values range from -9.1‰ to 2.3‰ across sections (Figure 4). Values steadily increase throughout all sections, except for a dramatic spike to more positive values at the top of Borcher's 3 and near the bottom of the section Borcher's 4. The Levene's test for unequal variances in the $\delta^{18}O_w$ values among sections ($F_{6, 35}$= 4.1196, p=0.0031). Both the Welch's nonparametric test and one-way ANOVA ($F_{6, 12.146}$=25.328, P<0.001) were highly significant and in agreement, so we used the Tukey-Kramer post-hoc pairwise comparison test to interpret differences in mean $\delta^{18}O_w$ values among section (Table 1).

$\delta^{13}C$ values

Overall, there is a trend towards higher $\delta^{13}C$ values through time (Figure 5). $\delta^{13}C$ values range between -6.68‰ to 1.97‰ with an average standard error of 0.099‰ (Table 1). The Levene's test for $\delta^{13}C$ values across sections was not significant, but the one-way ANOVA was

highly significant ($F_{6, 12.2}$=29.09, P<0.0001). The Tukey-Kramer's post-hoc pairwise comparison separates the Meade Basin sections into three groups of sections. The NNT1 section has the highest variation with includes several distinct oscillations. Additionally, $\delta^{13}C$ values for the Wiens section are all outside the range of values for other sections.

Percent C_4 Calculations

$\delta^{13}C$ values were used to estimate the percent of the biomass that utilized the C_4 photosynthetic pathway ($\%C_4$) using the linear mixing model described by Fox et al. (2011b). The percent of C_4 biomass on the landscape increased from approximately 28% at ~5 m.y. to ~60% at 1.7 m.y. (Figure 6). The modern percent C_4 values for Meade Basin is 78% ± 10.8% (Fox et al., 2011a).

Weight Percent Carbonate

Weight percent carbonate ($wt\%_{carb}$) of the samples ranged between 36.1% and 90.9% (mean ~72%) (Table 1). $Wt\%_{carb}$ values were plotted against Δ_{47} temperature estimates, $\delta^{13}C$ values, and $\delta^{18}O_{water}$ values. No discernible relationships between these paleoenvironmental proxies and $wt\%_{carb}$ were observed (Figure 7).

Discussion

The last 65 million years has been a complex time for the Earth's climate (Beerling and Royer, 2011; Zachos et al., 2001), and high-resolution paleoenvironmental records from sites like the Meade Basin provide an unique opportunity to investigate the relative influences of local, regional, and global temperature and aridity patterns that are recorded in a well-preserved terrestrial record. By quantifying abiotic factors and biotic changes in the same record from the Meade Basin, we can gain novel insight into the interactions and dynamics that have shaped the development of the modern Great Plains grassland ecosystem. Here we show that Δ_{47} temperature estimates do not vary through time, and therefore, suggest that temperature may not have been the primary factor responsible for changes in vegetation and fauna between ~5 m.y. and ~2.5 m.y. Our results suggest that temperature was decoupled from changes in paleo-hydrology in the Meade Basin.

We used weight percent carbonate calculations to help to assess the likelihood that our temperature values reflects soil temperature, and not carbonate formed in other settings or after soil formation. The majority of the samples analysed have high weight percent carbonate values and morphologies consistent with soil carbonate nodules, which indicate that the carbonate formed from soil processes (Snell et al., 2013). Our visual assessment of bivariate scatterplots of weight percent carbonate values versus $\delta^{18}O_w$ and $\delta^{13}C$ values found no correlation (Figure 7). This suggests that the lower weight percent carbonate samples, which are less reliably derived from soil processes than the higher weight percent carbonate samples, were derived from a similar fluid source as the more reliable, higher weight percent carbonate samples.

Samples with Δ_{48}-excess have been plotted separately in order to assess if there is a relationship between Δ_{48}-excess and the paleoenvironmental proxies (Figure 7). For all the plots,

data with Δ_{48}-excess are consistently the outliers of the general data cluster. This indicates that upon further sample and replicate analysis, data with Δ_{48}-excess could potentially be winnowed out of the overall data set in an attempt to provide a cleaner signal for $\delta^{18}O_w$, $\delta^{13}C$, and Δ_{47} temperature values.

Although Δ_{47} temperature estimates do not vary among sections, they do vary within sections. This variability may result from a number of factors. First, temperature estimates derived from soil carbonate nodules often show a warm-season bias in formation timing (Hough et al., 2014; Quade et al., 2012; Passey et al., 2010; Breecker et al., 2009). Based on these studies, we infer that our temperature estimates reflect summer temperatures. Second, clumped isotope temperature estimates that are derived from soil carbonate nodules may produce temperatures estimates that are higher than mean summer air temperatures, due in part to solar heating at the surface when ground cover is low (Hough et al., 2014). Third, as discussed in Quade et al. (2012), the depth of formation may also have a significant impact on the Δ_{47} temperature estimates, if samples have been collected from various depths in a soil horizon. At deeper depths in the soil profile, temperatures are less affected by seasonal and diurnal cycles, and therefore, nodules that form during the summer will be cooler at greater depths in the soil profile. Ground surface heating and potential site shading must be considered when examining temperature estimates. Much of the variation in temperature estimates is attributed to a combination of these phenomena. In section NNT1, we believe that more detailed sampling has captured a record that demonstrates the variation in temperature that occurs due to carbonate burial depth. There appears to be two distinct soil horizons within NNT1, as shown by two obvious oscillations from cooler to warmer temperatures (Figure 3).

$\delta^{18}O_w$ values do vary among sections and further analyses and replicates are needed to understand in-section trends and potential outliers. The enrichment of $\delta^{18}O_{water}$ values suggests increased evaporation, possibly as a product of increased aridity. In addition, an increase in $\delta^{18}O$ values may reflect the effects of the onset of continental glaciation, which increases $\delta^{18}O$ values of the starting moisture source (Fox et al., 2011b).

This study provides an additional data set to examine the evolution of C_4 grasses in the Meade Basin, complementing previous work conducted by Fox et al. (2011a). Statistical analysis finds that $\delta^{13}C$ values change through time, which may reflect a change in the percent of C_4 biomass on the landscape. The steady increase in the percent of C_4 biomass on the landscape is in agreement with previously reported percent C_4 estimates by Fox et al (2011a). Fox et al. (2011a) report that the first appearance of an ecosystem like that of the modern Great Plains, in regards to the abundance of C_4 grasses, occurred between 1.47-1.23 Ma. Variations in section, particularly for section Wiens, could reflect local paleoenvironmental differences, such as heterogeneity of vegetation or potential diagenesis. We have shown that temperature does not change over time and so temperature and temporal changes in paleovegetation do not correlate.

Conclusions

The Meade Basin is an ideal example of a Great Plains grassland ecosystem, and the basin has also provided well-preserved and well-understood paleoenvironmental records. Using "clumped" isotope paleothermometry and stable isotope geochemistry, we have begun to unveil the complex interactions between abiotic and biotic factors across this landscape. Throughout the 5 to 2.5 m.y. record that was analysed for this project, temperature estimates do not vary systematically through time, but do have unequal variances within individual sections. $\delta^{18}O_w$ values increase overtime suggesting that aridification may have played a role in the evolution of the Meade Basin ecosystem. $\delta^{13}C$ values also increase temporally indicating a steady increase in the percent of the biomass on the landscape that is C_4 grasses. The results of this study indicate that temperature is not likely the driving factor that has caused the rapid expansion of this C_4 dominated ecosystem in the Meade Basin. To further understand the effect of temperature on the evolution of the modern Great Plains grassland ecosystem, more samples and replicates need to be analysed in order to produce a more comprehensive and robust paleotemperature and paleovegetation record.

Based on our current results, we are unable to attribute this massive ecosystem shift to changes in paleotemperature; therefore, other factors must also be examined in order to develop a comprehensive picture of this ecosystem through time. Several partner projects are currently underway and aim to assess the roles of mean annual precipitation and organic biomarker records in the paleoenvironment. As we face rapid climate change across the globe, understanding the evolution of the Great Plains ecosystem in greater detail may provide insight into other complex ecosystems and future environmental shifts and changes.

Acknowledgements

First and foremost, I would like to thank Professor Kena Fox-Dobbs of the Geology Department for the thoughtful and enthusiastic guidance and mentorship that she has given me during my time at the University of Puget Sound. She sparked my interest in biogeochemistry, has provided me with amazing opportunities, and has consistently motivated me to strive for new and diverse academic achievements. I would like to also thank Professor Kathryn Snell for her expertise and patient guidance as she introduced me to clumped isotope paleothermometry at the California Institute of Technology and coached me through data analysis and interpretation. Additionally, I would like to thank the other primary investigators associated with this project: Professor David Fox, Dr. Pratigya Polissar, and Dr. Kevin Uno for their input and expertise. Thank you to all of those who we involved in the field team in Meade Basin. In particular, thank you to Elizabeth Roepke and Brenden Femal for their partnership and being on 'Team Rat' with me. Finally, I would like to the thank the University of Puget Sound, the Geology Department, and the Coolidge Otis Chapman Honors Scholar Program for the many opportunities for academic and personal growth that have been afforded me over my four incredible years at Puget Sound and my wonderful family for supporting me along the way.

References

Beerling, D.J. and Royer, D.L. 2011. Convergent Cenozoic CO_2 history. Nature Geoscience. 4, 418-420.

Bowen G. J. and Revenaugh J. 2003. Interpolating the isotopic composition of modern meteoric precipitation. Water Resources Research 39(10), 1299.

Bremer, K. 2002. Gondwanan evolution of the grass alliance of families (Poales): Evolution; International Journal of Organic Evolution. 121, 630-640.

Breecker, D.O., Sharp, Z.D., and McFadden, L.D.. 2010. Atmospheric CO_2 concentrations during ancient greenhouse climates were similar to those predicted for A.D. 2100. Proceedings of the National Academy of Science, USA. 107, 576-580.

Breecker, D.O., Sharp, Z.D., and McFadden, L.D. 2010. Seasonal bias in the formation and stable isotopic composition of pedogenic carbonate in modern soils from central New Mexico. Geological Society of America Bulletin. 121 (3/4), 630-640.

Cerling, T.E., Wynn, J.G., Andanje, S.A., Bird, M.I., Korir, D.k>, Levin, N.E., Mace, W., Macharia, A.N., Quade, J., and Remien, C.H. 2011. Woody cover and hominin environments in the past 6-million years. Nature, 475, 51-56.

Cerling, T.E. and Quade, J. 1993. Stable Isotopes in Soil Carbonates. Climate Change in American Geophysical Union, Geophysical Monograph 78, 217-231.

Cerling, T.E., Harris, J.M., MacFadden, B.J., Leakey, M.G., Quade, J., Eisenmann, V., Ehleringer, J.R. 1997. Global vegetation change through the Miocene/Pliocene boundary. Nature. 389, 153-158.

Christin, P.A., Besnard, G., Samaritani, E., Duvall, M.R., Hodkinson, T.R., Savolainen, V., and Salamin, N. 2008. Oligocene CO_2 decline promoted C_4 photosynthesis in grasses. Current Biology. 18. 37-43.

Cowling, S.A., Jones, C.D., and Cox, P.M. 2007. Consequences of the evolution of the C4 photosynthesis for surface energy and water exchange. Journal of Geophysical Research. 112, G01020.

Edwards, G.R., Osborne, C.P., Str□mberg, C.A.E., Smith, S.A., and the C_4 Grasses Consortium. 2010. The origins of C_4 grasslands: Integrating evolutionary and ecosystem science. Science. 328, 587-591.

Edwards, E.J. and Smith, S.A. 2010. Phylogenetic analyses reveal the shady history of C_4 grasses. Proceedings of the National Academy of Sciences USA. 107, 2532-2537.

Eiler, J.M., 2007. “Clumped-isotope” geochemistry – The study of naturally-occurring, multiply-substituted isotopologues. Earth and Planetary Science Letters. 262, 309–327.

Eiler, J.M., Schauble,E., 2004. (OCO)–O18–C13–O16 in Earth's atmosphere. Geochim. Cosmochim. Acta 68, 4767–4777.

Ehleringer, J.R., Cerling, T.E., Helliker, B.R. 1997. C_4 photosynthesis, atmospheric CO_2, and climate. Oecologia. 112, 285-299.

Ehleringer, J.R., Sage, R.F., Flanagan, L.B., and Pearcy, R.W. 1991. Climate change and the evolution of C_4 photosynthesis: Trends in Ecology & Evolution, 6, 95-99.

Fox, D.L., Honey, J.G., Martin, R.A., and Peláez-Campomanes, P., 2012b, Pedogenic carbonate stable isotope record of environmental change during the Neogene in the southern Great Plains, southwest Kansas, USA: Carbon isotopes and the evolution of C_4-dominated grasslands. Bulletin Geological Society of America. 124, 444-462.

Fox, D.L., Honey, J.G., Martin, R.A., Peláez-Campomanes, P., 2012. Pedogenic carbonate stable isotope record of environmental change during the Neogene in the southern Great Plains, southwest Kansas, USA: Oxygen isotopes and paleoclimate during the evolution of C_4-dominated grasslands. Bulletin Geological Society of America. 124, 431-443.

Fox, D.L., and Koch, P.L. 2003. Carbon and oxygen isotopic variability in Neogene paleosol carbonates: Constraints on the evolution of the C_4-dominated grasslands of the Great Plains, USA. Paleogeography, Palaeoclimatology, Palaeoecology, 207, 305-329.

Fox, D.L. and Koch, P.L. 2003. Tertiary history of C_4 biomass in the Great Plains, USA. Geology, 31, 809-812.

Ghosh, P., Adkins, J., Affek, H., Balta, B., Guo, W.F., Schauble, E.A., Schrag, D., Eiler, J.M., 2006. C13–O18bonds in carbonate minerals: A new kind of paleothermometer. Geochim. Cosmochim. Acta70, 1439–1456.

Hibbard, C.W. and Taylor, D.W., 1960. Two late Pleistocene faunas from southwestern Kansas. Contributions Museum of Palaeontology, University of Michigan, 56, 1-223.

Hough, B.G., Fan, M., Passey, B.H., 2014.Calibration of the clumped isotope geothermometer in soil carbonate in Wyoming and Nebraska, USA: Implication for paleoelevation and paleoclimate reconstruction. Earth and Planetary Science Letters, 391, 110-120.

Huntington, K.W., Eiler, J.M., Affek, H.P., Guo, W., Bonifacie, M., Yeung, L.Y., Thiagarajan, N., Passey, B., Tripati, A., Daeron, M., and Came, R. 2009. Methods and limitations of 'clumped' CO_2 isotope Δ_{47} analysis by gas-source isotope ratio mass spectrometry. Journal of Mass Spectrometry. 44, 1318-1329.

Izett, G.A. and Honey, J.G., 1995. Geologic map of the Irish Flats NE quadrangle, Meade Country, Kansas, United States Geologic Survey Miscellaneous Investigations Series Map I-2498.

Janssen, T., and Bremer, K., 2004. The age of major mococot groups inferred from 800+ rbcL sequences. Botanical Journal of the Linnean Society. 146, 385-398.

Latorre, C., Quade, J., McIntosh, W.C., 1996. The expansion of C_4 grasses and global change in the late Miocene: Stable isotope evidence from the Americas, Earth and Planetary Science Letters, 146, 83-96.

Martin, R.A., Honey, J.G., and Peláez-Campomanes, P., 2000, The Meade Basin rodent project: A progress report: Paludicola. 3, 1–32.

Martin, R.A., Peláez-Campomanes, P., Honey, J.G., Fox, D.L., Zakrzewski, R.J., Albright, L.B., Lindsay, E.H., Opdyke, N.D., and Goodwin, H.T., 2008. Rodent community change at the Pliocene-Pleistocene transition in south western Kansas and identification of the Microtus immigration event on the Central Great Plains. Palaeogeography, Palaeoclimatology, Palaeoecology. 267, 196–207.

McInerney, F.A., Str□mberg, C.A.E., and White, J.W.C., 2011. The Neogene transition from C_3 to C_4 grasslands in North America: stable carbon isotope ratios for fossil phytoliths. Paleobiology. 37(1), 23-49.

Passey, B.H., Levin, N.E., Cerling, T.E., Brown, F.H., Eiler, J.M., 2010. High-temperature environments of human evolution in East Africa based on bond ordering in paleosol carbonates. Proc. Natl. Acad. Sci. USA 107, 11245–11249.

Passey, B.H., Cerling, T.E., Perkins, M.E., Voorhies, M.R., Harris, J.M., and Tucker, S.T. 2002. Environmental change in the Great Plains: An isotopic record from fossil horses. Journal of Geology. 110, 123-140.

Prasad, V., Str□mberg, C.A.E., Alimohammadian, H., and Sahni, A., 2005. Dinosaur coprolites and the early evolution of grasses and grazers. Science. 30, 1177-1180.

Quade, J., Eiler, J., Daëron, M., Achyuthan, H., 2013. The clumped isotope geothermometer in soil and paleosol carbonate. Geochim. Cosmochim. Acta 105, 92.

Sage, R.F. 2004. The evolution of C_4 photosynthesis. The New Phytologist. 161. 341-370.

Still, C.J., Berry, J.A., Collatz, G.J., and DeFries, R.S. 2003. Global distribution of C-3 and C-4 vegetation: Carbon cycle implications. Global Biogeochemical Cycles. 17, 1-14.

Snell, K.E., Thrasher, B.L., Eiler, J.M., Koch, P.L., Sloan, L.C., and Tabor, N.J. 2013. Hot summers in the Bighorn Basin during the early Paleogene. Geology. 41, 55-58.

Str□mberg, C.A.E. and McInerney, F.A. 2011. The Neogene transition from C_3 to C_4 grasslands in North America: Assemblage analysis fossil phytoliths. Paleobiology. 37, 50-71.

Swart, P.K., Burns, S.J., Leder, J.J., 1991. Fractionation of the stable isotopes of oxygen and carbon in carbon-dioxide during the reaction of calcite with phosphoric-acid as a function of temperature and technique. Chemical Geology. 86, 89–96.

Tipple, B.J., Meyers, S.R., and Pagani, M. 2010. Carbon isotope ratio of Cenozoic CO_2: A comparative evaluation of available geochemical proxies. Paleooceanography. 25, PA3202.

Tipple, B.J., and Pagani, M. 2007. The early origins of terrestrial C_4 photosynthesis. Annual Review of Earth and Planetary Sciences. 35. 435-461.

von Fischer, J.C., Tieszen, L.L., and Schimel, D.S. 2008. Climate controls on C_3 vs. C_4 productivity in North American grasslands from carbon isotope composition of soil organic matter. Global Change Biology. 14, 1141-1155.

Wang, Z.G., Schauble, E.A., Eiler, J.M., 2004. Equilibrium thermodynamics of multi-ply substituted isotopologues of molecular gases. Geochim. Cosmochim. Acta 68, 4779–4797.

Zakrzewski, R.J. 1975. Pleistocene stratigraphy and paleontology in western Kansas: the state of the art. Studies on Cenozoic Paleoontology and stratigraphy in honor of Claude W. Hibbard. University of Michigan. Papers on Paleoontology, 12.

Appendix I: Figures

Figure 1: Site map of Meade Basin, Kansas modified from Fox et al. (2011a/b). Section locations are marked individually. On the north side of the Cimarron River, site locations have very similar geographic locations and so in order to distinguish sites visually distances between sites have been slightly exaggerated.

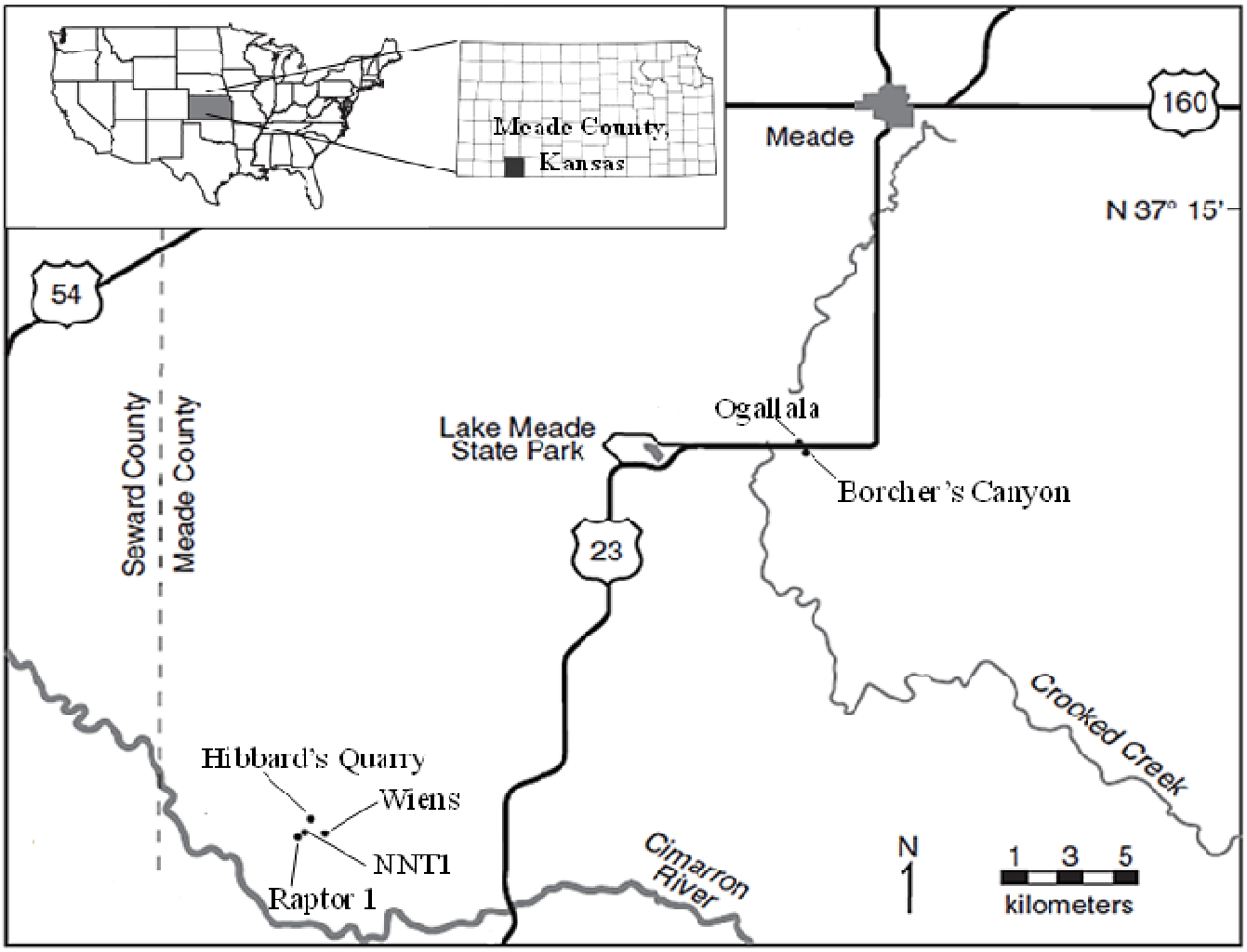

Figure 2. Composite stratigraphic summary of the seven sections analyzed in this study from the Meade Basin. Original stratigraphic column has been modified from Fox et al. (2011a). NALMA: North American Land Mammal Age.

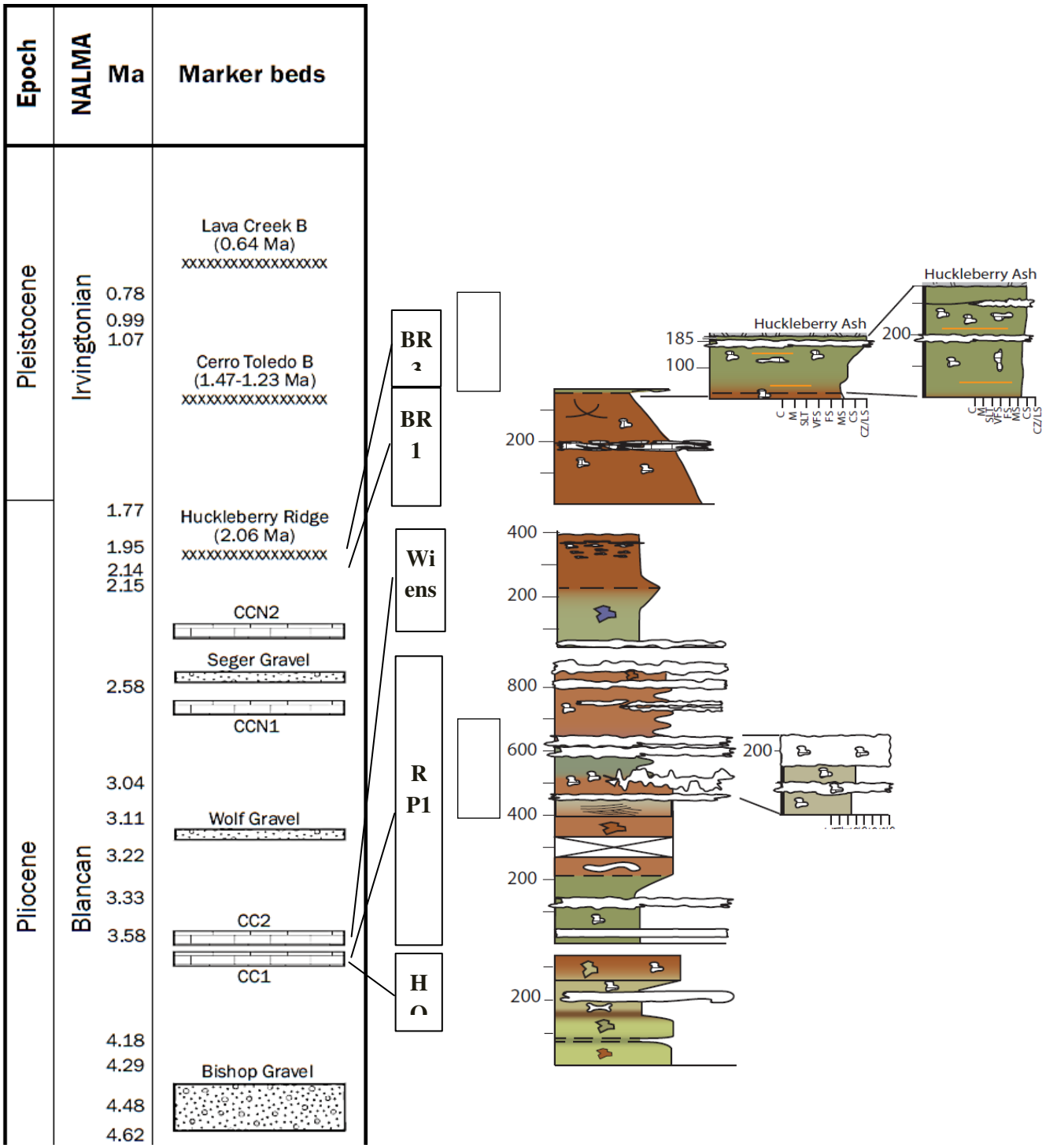

Figure 3: Estimated temperature (□C) calculated from Δ_{47} values of paleosol carbonate nodules. The dashed vertical line indicates the average temperature, 21.4°C, and the light grey shaded box includes ± 1 standard deviation (5°C). Modern mean annual (MAT, 14□C) and mean warm season (MWST, 24□C) temperatures are indicated with labelled dotted lines. Two ages are based upon marker beds; Huckleberry Ridge Ash (2.06 Ma) and CC1 (3.6 Ma), indicated by the horizontal, long dashed lines (Fox et al., 2011a; Martin et al., 2003).

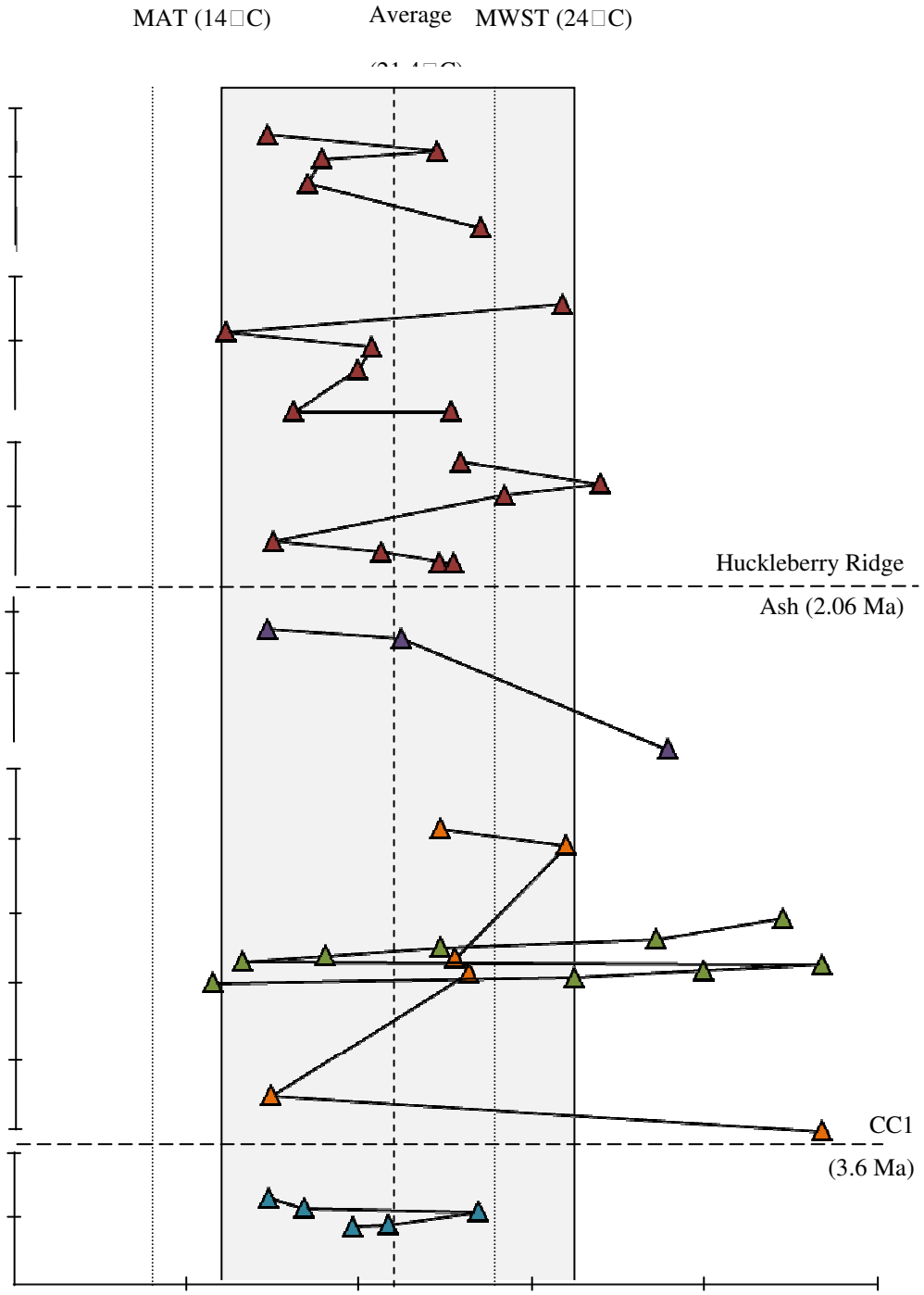

Figure 4: $\delta^{18}O$ values of water (SMOW) of paleosol carbonate nodules plotted relative to in-section stratigraphic height. Two ages are based upon marker beds; Huckleberry Ridge Ash (2.06 Ma) and CC1 (3.6 Ma), indicated by the horizontal, long dashed lines (Fox et al., 2011a; Martin et al., 2003). The estimated modern warm season $\delta^{18}O_{water}$ value (-6.675‰) for precipitation in Meade Basin is shown using a vertical dotted line and was calculated using the Online Isotopes in Precipitation Calculator (version 7.2008) (Lat: 37.28, Long: 100.339, Alt: 762m, avg. of May-Aug) (Bowen and Revenaugh, 2003).

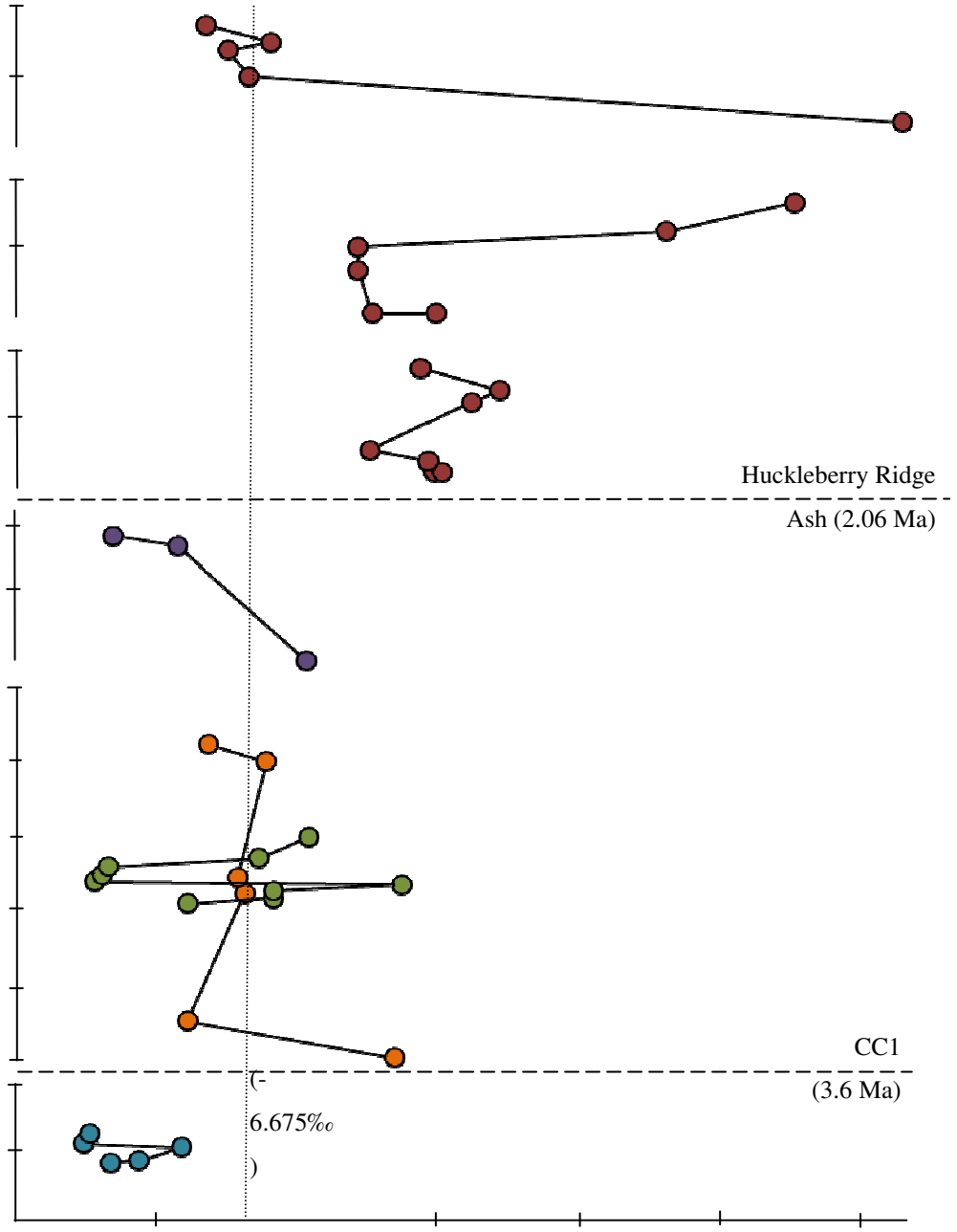

Figure 5: $\delta^{13}C$ values (VPDB) of paleosol carbonate nodules are plotted relative to in-section stratigraphic height. Two ages are based upon marker beds; Huckleberry Ridge Ash (2.06 Ma) and CC1 (3.6 Ma), indicated by the horizontal, long dashed lines (Fox et al., 2011a; Martin et al., 2003). The modern mean $\delta^{13}C$ value ± 1 standard deviation for 20 Holocene paleosol carbonates from arid-climate pure-C_3 plant ecosystems is 8.0‰ (Fox et al., 2011a).

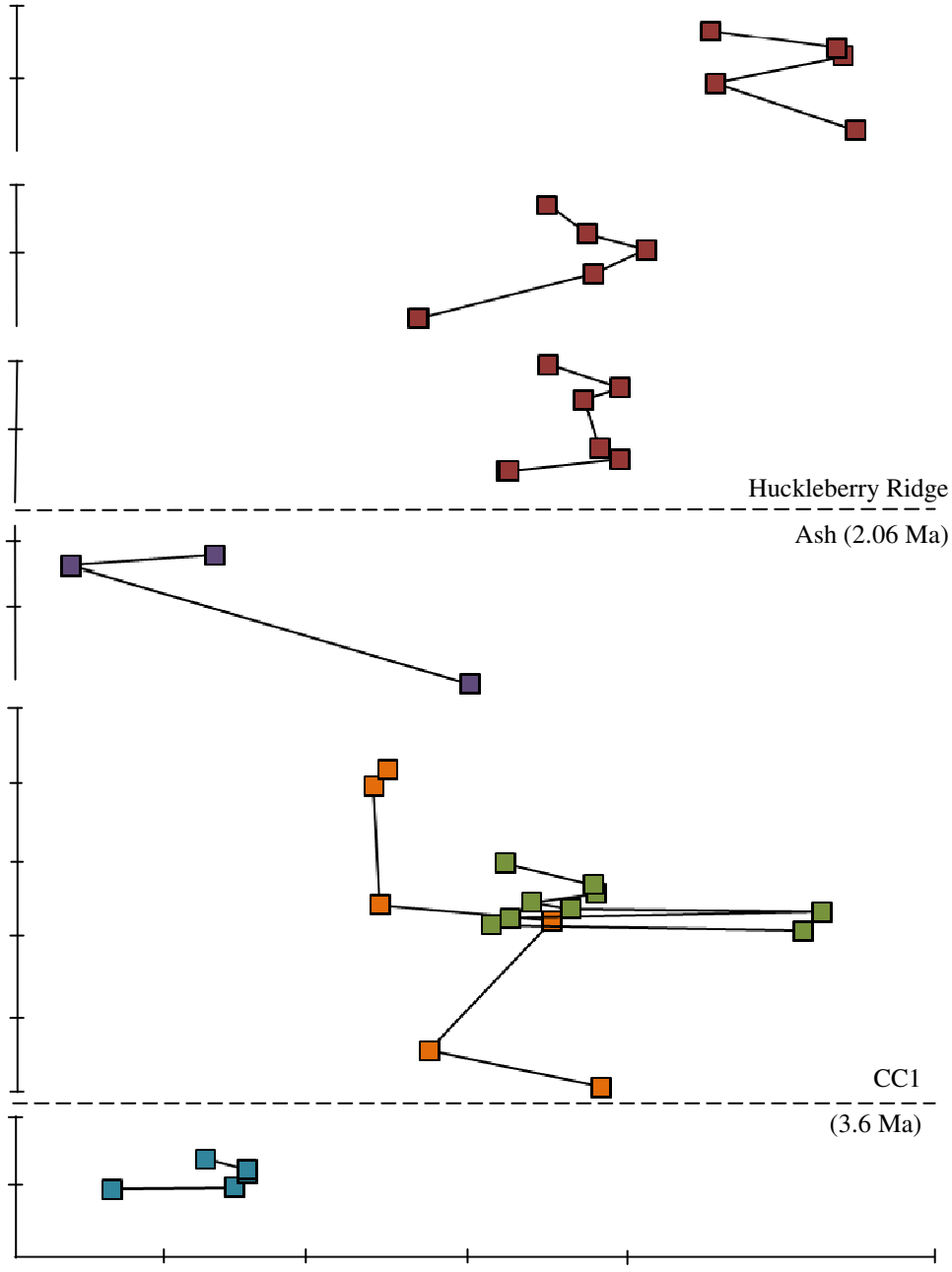

Figure 6: Percent C_4 biomass on the landscape calculated from paleosol carbonate nodule $\delta^{13}C$ values following Fox et al. (2011a). Dashed line and light grey box indicate mean modern abundance of C_4 biomass in the Meade Basin region ± 1 standard deviation. Data is plotted relative to in-section stratigraphic height. Two ages are based upon marker beds; Huckleberry Ridge Ash (2.06 Ma) and CC1 (3.6 Ma), indicated by the horizontal, long dashed lines (Fox et al., 2011a; Martin et al., 2003).

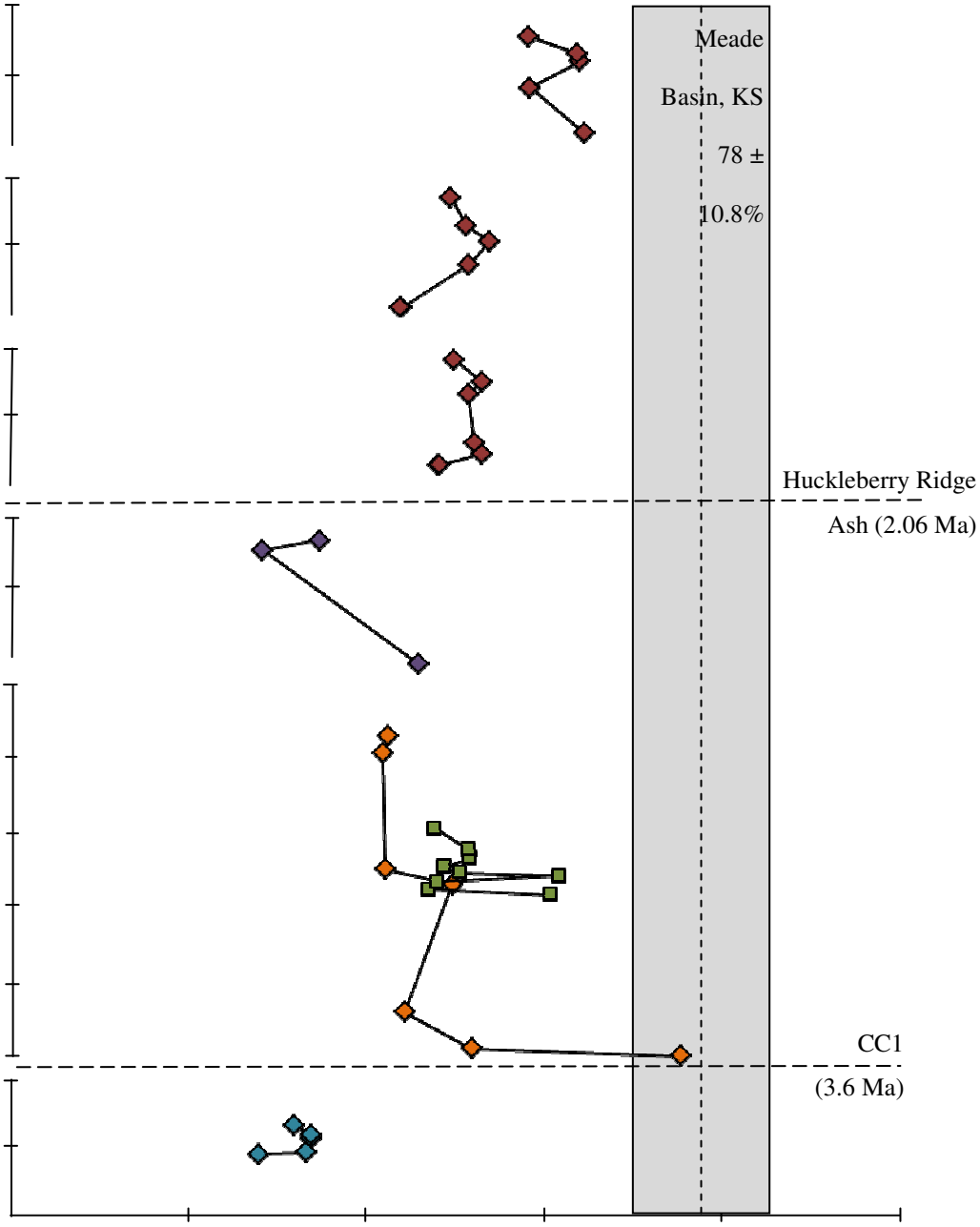

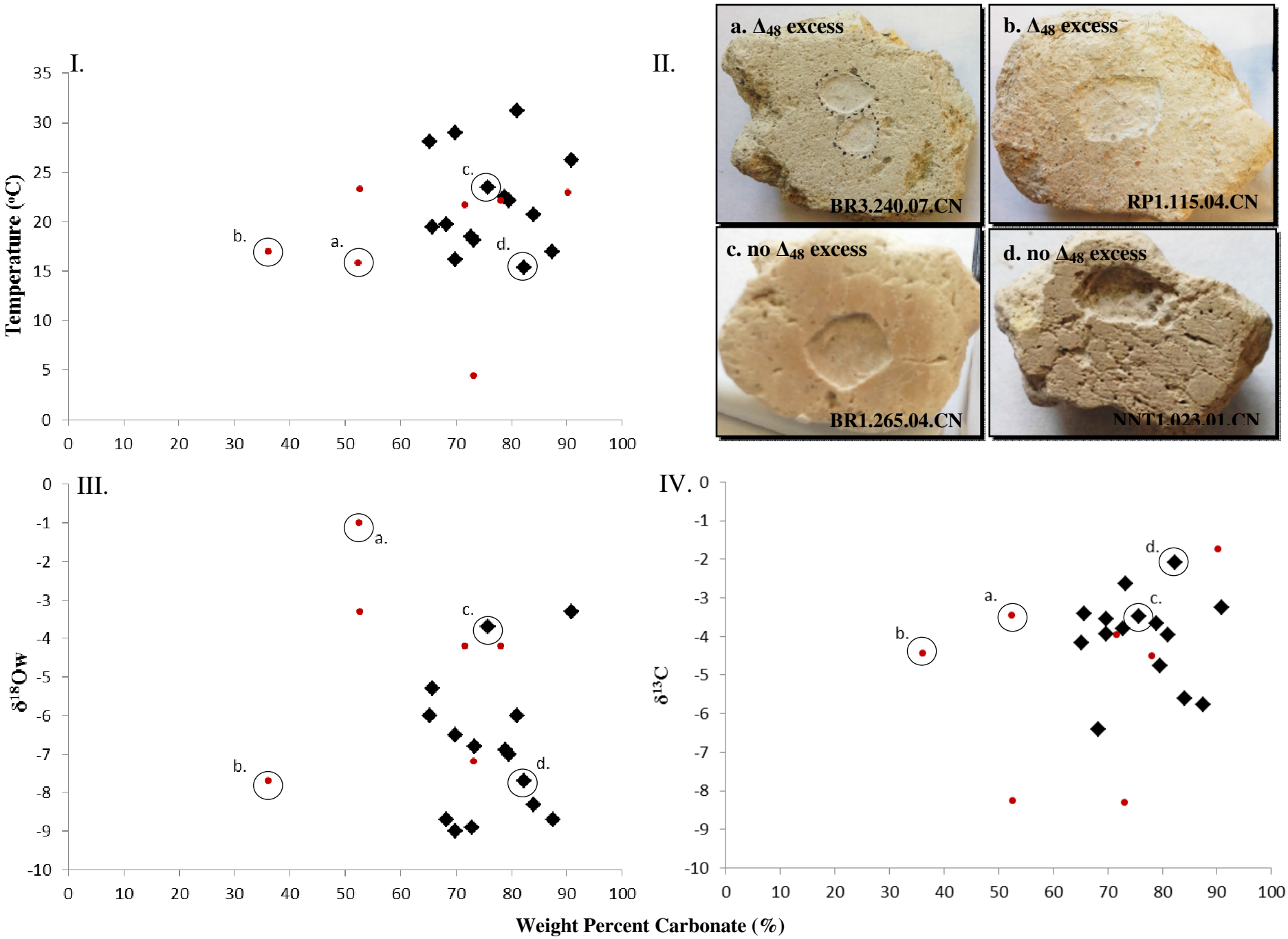

Figure 7: Weight percent carbonate in paleosol carbonate nodules was calculated in reference to 100% carbonate standards and is shown against I.) temperature estimates (□C), III.) $\delta^{18}O_{water}$ values, and IV.) $\delta^{13}C$ values. The black diamonds indicate samples that do not have excess mass-48 (Δ_{48} excess), while small red circles indicate samples that have Δ_{48} excess, as determined by Caltech inter-lab standards. Quadrant II demonstrates the variety of carbonate nodules sampled throughout the sections and each sample letter correlates to the data point in the plots in I, III, and IV. Drill sites on each sample demonstrate to what extent and to what depth each sample was drilled.

Appendix II: Tables

Table 1. Summary of Δ_{47}, temperature estimates, $\delta^{18}O_w$, weight percent carbonate, and percent C_4 biomass. Stratigraphic height is measured for each section from the local datum. Sections means are given for temperature estimates, $\delta^{13}C$, and $\delta^{18}O$, and statistically-derived group distinctions are indicated with a subscripted letter to demonstrate significant differences between sites.

Sample ID	Strat. Height (cm)	Δ_{47} (avg)	Δ_{47} (1 s.e.)	Section Mean T (□C)	T (□C)	T (□C) (1 s.e.)	Section Mean $\delta^{13}C$ (‰)	$\delta^{13}C_c$ (‰,PDB)	$\delta^{13}C_c$ (1s.e.)	Section Mean $\delta^{18}O_w$ (‰)	$\delta^{18}O_w$ (‰, SMOW)	$\delta^{18}O_w$ (1 s.e.)	Weight $\%_{Carb}$	% C_4
Borcher's 4														
BR4.070.03.CN	70	0.721	0.001	19.640	22.9	2.4	-2.148_A	-1.75	0.008	$-5.100_{A, B, C}$	2.3	0.5	90.2	61.4
BR4.190.05.CN	190	0.745	NA		18.1	NA		-2.63	Inf		-6.8	NA	73.3	55.5
BR4.260.07.CN	260	0.743	NA		18.5	NA		-1.83	NA		-7.1	NA	NA	60.9
BR4.280.08.CN	280	0.727	Inf		21.7	Inf		-1.87	NA		-6.5	NA	NA	60.6
BR4.325.10.CN	325	0.751	NA		17	NA		-2.66	NA		-7.4	NA	NA	55.3
Borcher's 3														
BR3.025.01.CN	25	0.725	0.022	20.033	22.1	5.4	$-3.775_{A, B}$	-4.5	0.001	-3.350_A	-4.2	1.1	78.2	41.6
BR3.025.01.CN	25	0.747	0.003		17.7	2.7		-4.51	0.077		-5.1	0.6	NA	41.5
BR3.140.04.CN	140	0.738	0.009		19.5	3.2		-3.41	0.004		-5.3	0.7	65.8	48.9
BR3.200.06.CN	200	0.736	NA		19.9	NA		-3.08	NA		-5.3	NA	NA	51.1
BR3.240.07.CN	240	0.757	NA		15.8	NA		-3.45	NA		-1	NA	52.5	48.7
BR3.315.10.CN	315	0.71	NA		25.2	NA		-3.7	NA		0.8	NA	NA	47.0
Borcher's 1														
BR1.080.10.CN	80	0.727	NA	21.857	21.7	NA	$-3.567_{A, B}$	-3.96	NA	$-4.157_{A, B}$	-4.2	NA	71.7	45.2
BR1.080.10.CN	80	0.725	NA		22.1	NA		-3.95	NA		-4.1	NA	NA	45.3
BR1.110.09.CN	110	0.735	NA		20.1	NA		-3.25	NA		-4.3	NA	NA	50.0
BR1.140.08.CN	140	0.75	NA		17.1	NA		-3.38	NA		-5.1	NA	NA	49.1
BR1.265.04.CN	265	0.718	0.019		23.5	4.8		-3.48	0.011		-3.7	1	75.7	48.5
BR1.295.03.CN	295	0.705	NA		26.2	NA		-3.25	NA		-3.3	NA	90.9	50.0
BR1.355.01.CN	355	0.724	0.011		22.3	3.4		-3.7	0.008		-4.4	0.7	NA	47.0
Wiens 1														
WI1.000.01.CN	0	0.696	0.025	21.933	28.1	6.2	$-5.540_{B, C}$	-4.17	0.013	$-7.500_{A, B, C}$	-6	1.2	65.3	43.2
WI1.300.03.CN	300	0.732	NA		20.7	NA		-6.68	NA		-7.8	NA	NA	26.3
WI1.325.05.CN	325	0.751	NA		17	NA		-5.77	NA		-8.7	NA	87.5	32.4
NNT1														
NNT1.023.01.CN	23	0.759	0.004	24.156	15.4	2.9	-3.350_A	-2.09	0.346	$-7.200_{B, C}$	-7.7	0.6	82.3	57.1
NNT1.038.03.CN	38	0.709	NA		25.4	NA		-4.05	NA		-6.5	NA	NA	44.0
NNT1.056.05.CN	56	0.692	0.041		29	9.8		-3.93	0.151		-6.5	1.9	69.8	44.8
NNT1.073.07.CN	73	0.677	NA		32.3	NA		-1.97	NA		-4.7	NA	NA	57.9
NNT1.080.08.CN	80	0.755	NA		16.2	NA		-3.55	Inf		-9	NA	69.8	47.3
NNT1.097.10.CN	97	0.743	0.013		18.5	3.8		-3.8	0		-8.9	0.8	72.8	45.6
NNT1.119.12.CN	119	0.727	NA		21.7	NA		-3.39	NA		-8.8	NA	NA	48.4
NNT1.142.14.CN	142	0.698	NA		27.7	NA		-3.41	Inf		-6.7	NA	NA	48.3
NNT1.197.19.CN	197	0.682	NA		31.2	NA		-3.96	NA		-6	NA	81.1	44.6

Raptor 1														
RP1.000.01.CN	0	0.75	Inf	22.557	17.1	Inf	$-3.673_{A, B}$	0	NA	$-7.057_{B, C}$	-9	NA	NA	71.1
RP1.020.02.CN	20	0.677	0.051		32.3	12.5		-3.36	0.004		-4.8	2.4	NA	48.6
RP1.115.04.CN	115	0.751	0.016		17	4.3		-4.44	0.03		-7.7	0.9	36.1	41.3
RP1.450.09.CN	450	0.723	0.017		22.5	4.5		-3.67	0.95		-6.9	0.9	78.9	46.5
RP1.490.13.CN	490	0.725	0.031		22.1	7.2		-4.75	0.003		-7	1.5	79.6	39.3
RP1.795.16.CN	795	0.71	NA		25.2	NA		-4.79	NA		-6.6	NA	NA	39.0
RP1.840.18.CN	840	0.727	NA		21.7	NA		-4.7	NA		-7.4	NA	NA	39.6
Hibbard's Quarry														
HQ1.185.15.CN	185	0.737	NA	-5.774	19.7	NA	-5.774_{C}	-6.4	NA	-8.560_{C}	-8.7	NA	68.2	28.2
HQ1.190.16.CN	190	0.732	0.026		20.7	6.1		-5.61	0.011		-8.3	1.3	84.1	33.5
HQ1.230.20.CN	230	0.719	0.031		23.3	7.3		-5.53	0.03		-7.7	1.5	NA	34.0
HQ1.240.21.CN	240	0.744	NA		18.3	NA		-5.53	NA		-9.1	NA	NA	34.0
HQ1.270.04.CN	270	0.749	NA		17.3	NA		-5.8	NA		-9	NA	NA	32.2